Nitrogen-enhanced indium segregation in (Ga,In)(N,As)/GaAs multiple quantum wells grown by molecular-beam epitaxy

New Journal of Physics
The open-access journal for physics

Nitrogen-enhanced indium segregation in (Ga,In)(N,As)/GaAs multiple quantum wells grown by molecular-beam epitaxy

E Luna[1,4], A Trampert[1], E-M Pavelescu[2,3] and M Pessa[2]

[1] Paul-Drude Institute for Solid State Electronics, Hausvogteiplatz 5-7, 10117 Berlin, Germany

[2] ORC, Tampere University of Technology, PO Box 692, FIN-33101 Tampere, Finland

E-mail: luna@pdi-berlin.de

New Journal of Physics **9** (2007) 405
Received 21 June 2007
Published 8 November 2007
Online at http://www.njp.org/
doi:10.1088/1367-2630/9/11/405

Abstract. Transmission electron microscopy (TEM) is used to determine the composition of quaternary (Ga,In)(N,As) quantum wells (QWs). Through a combined analysis of the chemically sensitive (002) dark-field (DF) images and the lattice-resolving high-resolution TEM images, the local distributions of nitrogen and indium in the growth direction are determined. In particular, we are able to directly detect the existence of indium segregation in (Ga,In)(N,As) QWs. A comparison with the indium distribution profile in the nitrogen-free (In,Ga)As QWs, grown under similar conditions, revealed that incorporating N into the alloy enhanced indium segregation.

[3] Present address: Technological Physics Group, University of Kassel, Heinrich Plett Strasse 40, D-34132 Kassel, Germany.

[4] Author to whom any correspondence should be addressed.

PII: S1367-2630(07)53301-X

Contents

1. Introduction

Dilute III–V-N heterostructures are of considerable research interest from both a fundamental and technological point of view [1, 2]. In particular, for the (Ga,In)(N,As) alloy, the huge band gap bowing by the introduction of N and the resulting strong redshift of the band gap, make it very attractive for application in GaAs-based laser diodes operating in the 1.3–1.55 μm optical fibre windows [3]–[5]. However, the mechanisms controlling the incorporation of In (35–40%) and N (2–5%) required for reaching the desired wavelength range are still not well understood [6]. It is accepted that the structural perfection of the alloy deteriorates dramatically with increasing N content due to the large miscibility gap and the phase separation tendency [7, 8]. As a consequence, composition fluctuations and interface undulations are generally developed, that can only be avoided by the growth at low temperatures ($T_g \leqslant 460\,^{\circ}$C) using techniques like molecular-beam epitaxy (MBE) [1]. On the other hand, realization of atomically flat and abrupt heterointerfaces is a matter of greatest concern. However, it is well known that during heteroepitaxial growth of (In,Ga)As, a considerable amount of indium atoms segregate to the surface [9]. As a consequence, spatially varying composition profiles appear that exert an undesirable influence on the optical and transport properties of superlattices and quantum wells (QWs) as they modify the intended potential profile and energy levels of the confined states [10]. Despite the fact that good performance (Ga,In)(N,As)-based lasers have been fabricated [6, 11], indium segregation in (Ga,In)(N,As) is a subject largely unexplored so far. Recently, it has been put forward that the presence of N in the alloy enhances In segregation [12]. This suggestion, however, is based on the data obtained from indirect experiments [12].

In this paper, we present direct experimental evidence of indium segregation in MBE-grown (Ga,In)(N,As) multiple-QWs by using transmission electron microscopy (TEM). MQWs are required to improve the performance of (Ga,In)(N,As) devices. In particular, the In and N compositions, [In] and [N], studied across the QWs were locally determined by a combined evaluation of the tetragonal lattice distortion of coherently strained structures and the contrast analysis of the chemically sensitive (002) dark-field (DF) TEM images [13]. The obtained profiles are then compared to those taken from nitrogen-free (In,Ga)As/GaAs QWs grown under similar conditions. For the T_g considered, we found that In segregation is undetectable in the (In,Ga)As MQWs, contrary to the (Ga,In)(N,As) case, where the presence of nitrogen promotes indium surface segregation.

2. Experimental

Ten 7-nm wide (Ga,In)(N,As) QWs with 30-nm thick GaAs potential-energy barriers were grown on GaAs(001) substrates under As-rich conditions in a MBE system equipped with a *rf* nitrogen plasma source. Prior to the growth of the (Ga,In)(N,As) MQWs, a 100 nm thick GaAs buffer layer was grown at 580 °C. The samples were prepared at two different growth temperatures $T_g = 420$ and 460 °C, measured by a thermocouple. For the growth of the MQW, the fluxes of all the elements were fixed throughout this study. Finally, a 100 nm GaAs cap layer was grown on top of the samples at the same temperature as the MQWs [14]. Growth took place in a layer-by-layer mode, as monitored by *in situ* reflection high-energy electron diffraction (RHEED). We examined two sets of samples. One of them contained (Ga,In)(N,As) QWs; the other contained QWs without nitrogen. The samples containing (Ga,In)(N,As) QWs are labelled G420 ($T_g = 420$ °C) and G460 ($T_g = 460$ °C). The corresponding (In,Ga)As samples are labelled I420 and I460. In all cases, we investigate the *as-grown* samples. Prior to the analysis by TEM, the samples were characterized by x-ray diffraction (XRD) and photoluminescence.

Cross-sectional TEM foils were prepared in the [110] and [$\bar{1}$10] projections, using mechanical thinning followed by Ar-ion milling. The TEM investigation was carried out using a Jeol JEM 3010 microscope operating at 300 kV, equipped with a GATAN CCD camera.

In classical ternary alloys (e.g. InGaAs and AlGaAs) there are two well-established techniques based on TEM to determine the composition: (i) measurement of the tetragonal lattice distortion from experimental high-resolution TEM (HR-TEM) or (ii) imaging and analysis of the intensity of the chemically sensitive (002) reflection from DF images. In the case of quaternary alloys, using only one of these methods give ambiguous results since a whole set of In and N concentrations leads to the same tetragonal distortion or DF intensity. Grillo *et al* [13] showed that the combined use of both methods solves the problem thus leading to an unambiguous and independent determination of the In and N content.

In III–V alloys, the diffracted intensity of the (002) reflection is proportional to the square of the (002) structure factor F_{002}, which depends on the difference in the atomic scattering factors, f, of the elements III and V [15]. In the case of the $Ga_{1-x}In_xN_yAs_{1-y}$ alloy, the kinematically diffracted intensity I_{002} can then be written as:

$$I_{002}^{(Ga,In)(N,As)} \propto [(f_{In} - f_{Ga})\,x + (f_{As} - f_N)\,y - (f_{As} - f_{Ga})]^2\,. \tag{1}$$

In order to avoid the necessity of measuring absolute intensities, the scattered intensity I_{002} of the (Ga,In)(N,As) QW is normalized to GaAs of the same thickness. The ratio R_{002} of the intensities of (Ga,In)(N,As) and GaAs is then a quadratic function of x and y:

$$R_{002} = \frac{I_{002}^{(Ga,In)(N,As)}}{I_{002}^{GaAs}} = f(x^2, y^2). \tag{2}$$

On the other hand, the coherent strain in the $Ga_{1-x}In_xN_yAs_{1-y}$ QWs, which depends on the composition as well [$a_\perp = f(x, y)$], produces a tetragonal distortion of the cubic unit cells that can directly be determined from the HR-TEM images. In our case, we use the LADIA program package [16] to evaluate the strain distribution. In short, this method is based on the local measurement of lattice spacing in HR-TEM micrographs, where the intensity maxima are identified related to the positions of atomic columns. The positions of these maxima are determined with respect to a reference lattice on the same micrograph. In our case, we use the GaAs barriers as a reference. The tetragonal lattice distortion of the layer is then the derivative of

the displacement between the atomic positions and the reference lattice [17]. The composition of the layer can then be calculated from the tetragonal distortion assuming Vegard's law, i.e. the tetragonal distortion depends linearly on the composition. The tetragonal lattice distortion of a (Ga,In)(N,As) layer on GaAs(001) is then:

$$\varepsilon(x, y) = \left(1 + \frac{2c_{12}^{(\mathrm{Ga,In})(\mathrm{N,As})}}{c_{11}^{(\mathrm{Ga,In})(\mathrm{N,As})}}\right) \frac{a_0^{(\mathrm{Ga,In})(\mathrm{N,As})} - a_0^{\mathrm{GaAs}}}{a_0^{\mathrm{GaAs}}}, \tag{3}$$

where $c_{ij}^{(\mathrm{Ga,In})(\mathrm{N,As})}$ are the elastic constants of the quaternary system, and $a_0^{(\mathrm{Ga,In})(\mathrm{N,As})}$ and a_0^{GaAs} are the lattice constants of the bulk alloy and substrate, respectively, which are obtained from the lattice parameter of the constituents (GaAs, GaN, InAs and InN) [18] assuming the validity of Vegard's law:

$$a_0^{(\mathrm{Ga,In})(\mathrm{N,As})} = (1-x)\left[(1-y)\, a_{\mathrm{GaAs}} + y a_{\mathrm{GaN}}\right] + x\left[(1-y)\, a_{\mathrm{InAs}} + y a_{\mathrm{InN}}\right]. \tag{4}$$

Estimates of the coefficients c_{ij} for (Ga,In)(N,As) are obtained from the corresponding binary constituents [18] assuming a linear interpolation:

$$c_{ij}^{(\mathrm{Ga,In})(\mathrm{N,As})} = (1-x)\left[(1-y)\, c_{ij}^{\mathrm{GaAs}} + y c_{ij}^{\mathrm{GaN}}\right] + x\left[(1-y)\, c_{ij}^{\mathrm{InAs}} + y c_{ij}^{\mathrm{InN}}\right]. \tag{5}$$

The combination of both techniques, the DF intensity and tetragonal distortion, i.e. solving equations (1)–(5) point by point across the QW, thus gives an unambiguous measurement of [In] and [N] as a function of the well depth. For the (In,Ga)As samples, [In] was directly determined from the analysis of the (002) DF images. In the analysis of the (002) images we took into account the atomic scattering factors given by Doyle and Turner [19], while influences of electron redistribution due to the bonding of atoms, local structural distortions and thin-foil surface relaxation [20]–[23] are not considered here. The analysis of the intensity of the (002) DF images is performed using the Digital Micrograph software (Digital Micrograph$^{\mathrm{TM}}$ Gatan, Inc.). For the determination of the intensity profile across the QW (Digital Micrograph) as well as of the strain distribution along the growth direction (LADIA) we performed several linescans averaged over an area 20×20 nm perpendicular to the QW. We then average the data of these *averaged-linescans* in order to further reduce the noise. We average the data coming from the same QW, but do not average the data coming from different QWs. The examination of several QWs confirms however that the results found are reproducible and do not depend on the selected QW. Figure 1(b) shows an averaged linescan of the contrast in the (002) DF images across a QW (figure 1(a)), the intensity being already normalized to that of GaAs. The average deviation of $I_{002}/I_{002}^{\mathrm{GaAs}}$ (R_{002}) in the GaAs barriers is $\sim$0.015 and this represents an estimate of the noise associated with this measurement. On the other hand, figure 1(c) shows the strain map obtained from the analysis of the HR-TEM images with LADIA, together with the strain distribution across a QW (figure 1(d)). In this case, the average deviation of the strain value in the GaAs barrier is $\sim$0.002, representing the estimated noise of this technique.

3. Results and discussion

3.1. Element distribution inside the (Ga,In)(N,As) QWs

Figures 2(a) and (b) show a cross-sectional (002) DF TEM micrograph for G420 and G460, respectively. As observed, in spite of the build-up of compressive strain, we have obtained morphologically perfect two-dimensional (2D) QWs. The QWs exhibit smooth interfaces, as

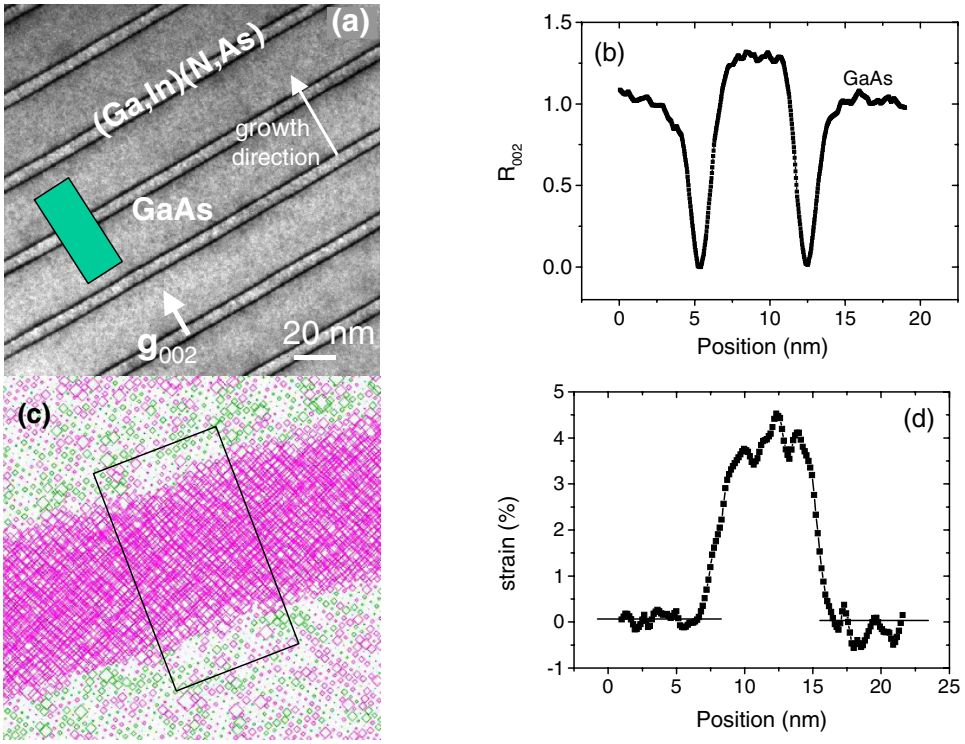

Figure 1. (a) $\mathbf{g}_{002}$ DF micrograph together with (b) an averaged linescan of the intensity normalized to that of GaAs. (c) Strain map obtained from the analysis of the HR-TEM images with LADIA. The symbol size is proportional to the strain value. (d) The corresponding strain distribution across a QW. The estimated noise of the techniques is obtained from the average deviation of the R_{002} and strain value, respectively, in the GaAs barrier.

indicated by the two dark lines on both sides of each QW, and laterally homogeneous overall composition. The origin for the two dark lines defining the interfaces is based upon the functional dependence of the intensity of the (002) reflection on the In and N concentrations [13, 24]. For a given N concentration, the (002) reflection intensity in kinematic approximation shows a parabolic behaviour with a minimum located in the range between 15 and 25% of In (the minimum of the parabola shifts with increasing N values to lower In concentration [13]). The intensity associated to the QWs studied here, containing about [In] = 40%, must therefore pass through a minimum at the interfaces, where the concentrations gradually drop down to zero, giving rise to the dark contrast.

As for the elemental distribution, figures 2(c) and (d) show the corresponding [In] and [N] profiles taken for G420 and G460. It turned out that the averaged [In] and [N] deduced from the experimental XRD data ([In] ∼41% and [N] ∼3.8%, after comparison with simulations, which were based on the dynamical diffraction theory [25]), deviated only about 2% for [In] and 1% for [N] from those attained from the TEM analyses. The error bars of the experimental element concentration obtained by the TEM analysis are about ±1.2% for In, and ±0.7% for N, that represent the standard deviation of the data after averaging.

While the In distribution inside the QW is rather homogeneous for G420, it has a pronounced asymmetry for G460, characteristic of segregation effects; i.e. the local indium

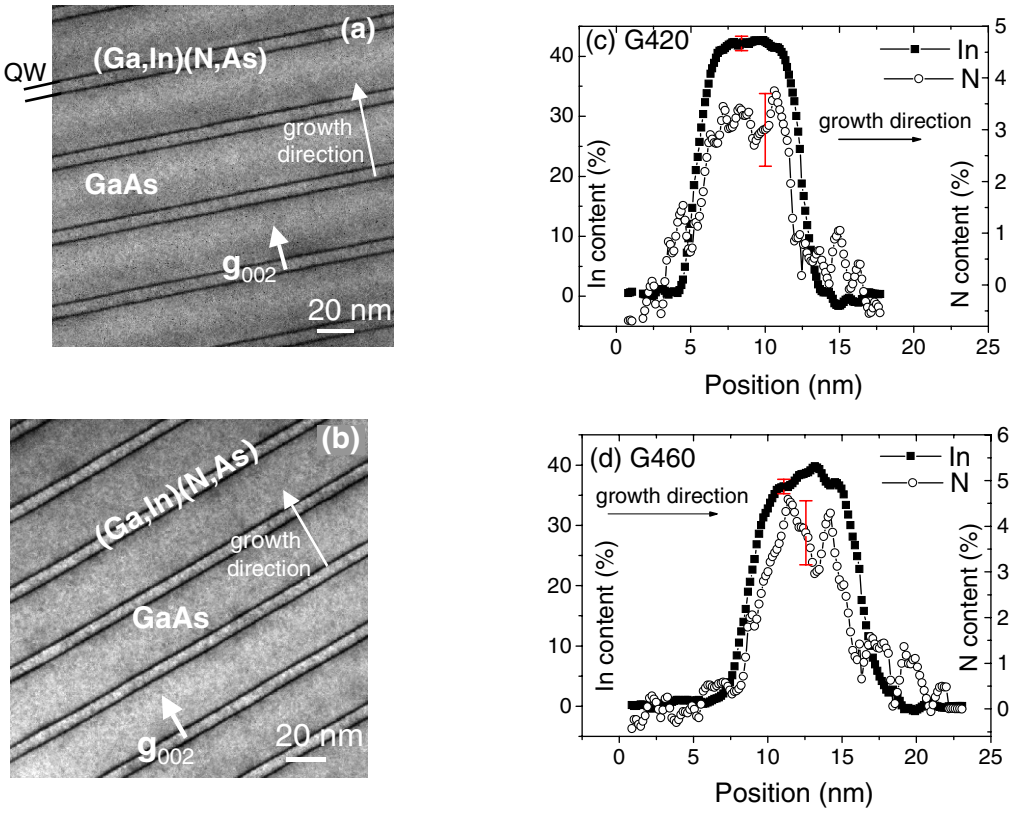

Figure 2. (a) $\mathbf{g}_{002}$ DF micrograph from sample G420, (b) G460. Experimental [In] and [N] profiles with error bars for (Ga,In)(N,As) QWs grown at (c) 420 °C and (d) 460 °C.

concentration gradually increases inside the QW, as growth proceeds. However, after the growth of the QW, hence after closing the indium shutter, we do not detect significant segregated indium into the upper GaAs barrier layer, which results in a rather symmetric distribution *at the interfaces*. Similar indium profiles are also found for other (Ga,In)(N,As) QWs [26].

The [N] profile of G460 exhibits a pronounced asymmetry, too. The areas of lower [N] correspond to the areas of higher [In], which is a well-known phenomenon caused by the preferred formation of Ga–N and In–As bonds with an increase in T_g, due to the phase separation tendency of the alloy [27]. For G460, the fluctuations in [N] are strong amounting to a difference of 1.6% between the minimum and maximum values in the QW. For G420 with reduced T_g, the fluctuations in [N] are only 0.8%.

3.2. Indium segregation in (Ga,In)(N,As)

The indium content across the (Ga,In)(N,As) QWs grown at 420 °C is homogeneous with a symmetric distribution profile, which can be well fitted by the error functions that describe diffusion processes (figure 3(a)):

$$x(n) = \frac{x_0}{2}\left[\operatorname{erf}\left(\frac{N_w + 2n}{4L}\right) + \operatorname{erf}\left(\frac{N_w - 2n}{4L}\right)\right], \tag{6}$$

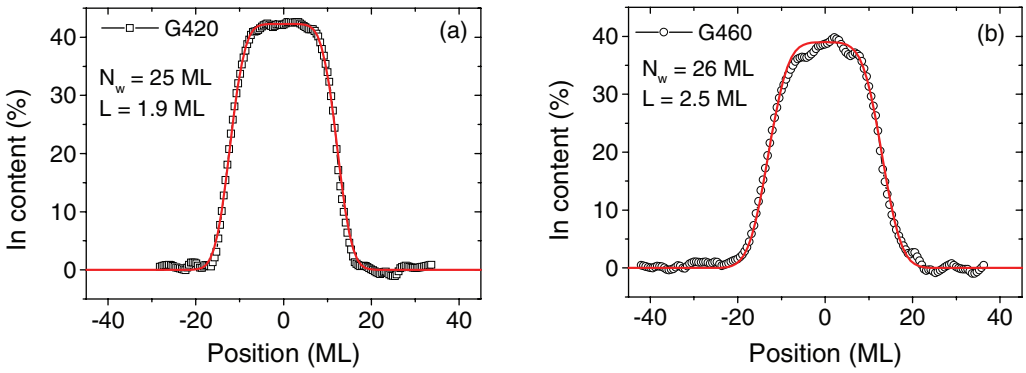

Figure 3. Experimental indium distribution from (a) G420 and (b) G460 described by error functions.

the composition profile is characterized by an interface roughness parameter, L [28]; x_0 is the nominal indium mole fraction, N_w is the well width in monolayers (ML), and n denotes the position along the growth direction.

The raise of T_g to 460 °C promotes a gradual increase in [In] from 36 to 40%, characteristic of In segregation. The question of how this increase in the In content with its consequent increase in strain might affect critical layer thickness (h_c) then arises. We have estimated the critical thickness using the Matthews and Blakeslee model [29] for 40% In and 3% N (the experimental In and N contents resulting from In segregation) and get $h_c \sim 19$ nm. This value is much lower than that obtained assuming 36% In and 4.6% N (before segregation), $h_c \sim 28$ nm. However, in spite of the reduction in h_c as a result of In segregation, our 7-nm wide QWs are still well below the estimated limit for plastic relaxation. This is in agreement with the experiments. We have evidence that the relaxation of epitaxial strain does not yet occur since no misfit dislocations were observed in the TEM investigations and the XRD data can be very well simulated assuming a coherently strained layer structure. Finally, it should be mentioned that, for a fixed indium content, the addition of nitrogen to the (In,Ga)As alloy compensates the high strain, thus increasing h_c as shown by Tomić and O'Reilly [30].

It is known that T_g is the growth parameter mainly controlling segregation and that increasing T_g increases indium segregation in (In,Ga)As [10]. We have found, however, that the impact of higher growth temperatures on In segregation in the (Ga,In)(N,As) QWs is partly masked by an increase in surface roughening and the appearance of lateral composition fluctuations [31]. Therefore, due to the phase separation tendency of (Ga,In)(N,As), the range of T_g to be explored is kept rather limited: on one side, the growth at higher T_g leads to severe morphological instabilities; and on the other, the lower the growth temperature is, the higher the point defects density and the larger the degradation of the optical properties.

In addition to the gradual increase in [In] inside the QW, the growth at $T_g = 460$ °C broadens the interfaces, if compared to G420 (figure 3). This can be explained by the enhanced thermally activated diffusion at the interfaces due to the increase of T_g. Similarly to G420, error functions also provide a good description at the interfaces of sample G460, as seen in figure 3(b), but in this case the [In] profile inside the QW clearly deviates from the symmetric fit.

Surface segregation of atoms is often described and quantified by a segregation efficiency factor, R, which defines the fraction of the topmost-layer atoms that move to the next layer. According to Muraki *et al*'s phenomenological model for segregation [10], the indium

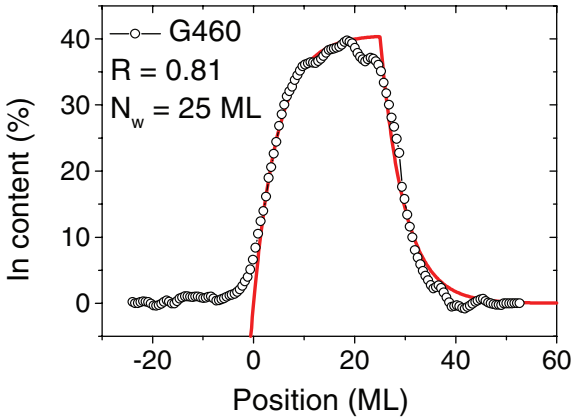

Figure 4. Fit to Muraki's model for segregation of the data plotted in figure 3(b).

concentration in the n-th ML is given by:

$$\begin{aligned} x_n &= x_0(1-R^n), \qquad (1 \leqslant n \leqslant N_\mathrm{w};\ \text{well}) \\ x_n &= x_0(1-R^{N\mathrm{w}})R^{n-N\mathrm{w}}, \qquad (n > N_\mathrm{w};\ \text{barrier}). \end{aligned} \tag{7}$$

In G460, a fit to Muraki's model for segregation (figure 4) yields $R = 0.81$; i.e. indium segregation is remarkable. For (In,Ga)As QWs, from the analysis of RHEED oscillations during MBE growth, Martini *et al* [32] found $R = 0.72$ at the same $T_\mathrm{g} = 460\,^\circ\mathrm{C}$; while a similar R of 0.8 has been reported for (In,Ga)As QWs grown at $T_\mathrm{g} = 535\,^\circ\mathrm{C}$ by lattice fringe analysis in the TEM by Litvinov *et al* [33].

Judging from our observations (figure 4), Muraki's model for segregation describes well the distribution of indium in the QW, but there is a discrepancy at the upper interface. As already mentioned, no significant 'tail' of indium atoms penetrates into the GaAs layer. Thus, it seems to be that interfaces act as a 'barrier' for segregation in this special material system.

3.3. Nitrogen-enhanced indium segregation

In order to explore the influence of nitrogen on indium segregation, we compared the In distribution obtained for the (In,Ga)As QWs grown under similar conditions (same T_g and element fluxes, but without N supply). We found that when growing them at $420\,^\circ\mathrm{C} \leqslant T_\mathrm{g} \leqslant 460\,^\circ\mathrm{C}$, indium segregation was undetectable, as shown in figure 5, and the [In] distribution is characterized by a diffusion-like symmetric profile. This is to say that indium segregation in the nitrogen-free QWs occurs at higher T_g's only. Figure 6 shows that [In] remains, indeed, constant at 39% across the QW (for I460), in contrast with the gradual increase in [In] for the sample with N in the QW (G460).

As deduced from the experiments, it is clear that the presence of nitrogen in the quaternary alloy enhances indium segregation. We attribute this effect to the increase in the driving force for segregation, i.e. higher elastic and bonding energy gradients [9], as a consequence of the introduction of nitrogen in (In,Ga)As. Due to the specific properties of the N atoms (small size and electronegativity), there are large differences in the bond lengths and cohesive energies between the arsenide-like and nitride-like 'environments' constituting the (Ga,In)(N,As) alloy [34] that makes the elastic and bonding energy gradients more pronounced than in the (In,Ga)As case.

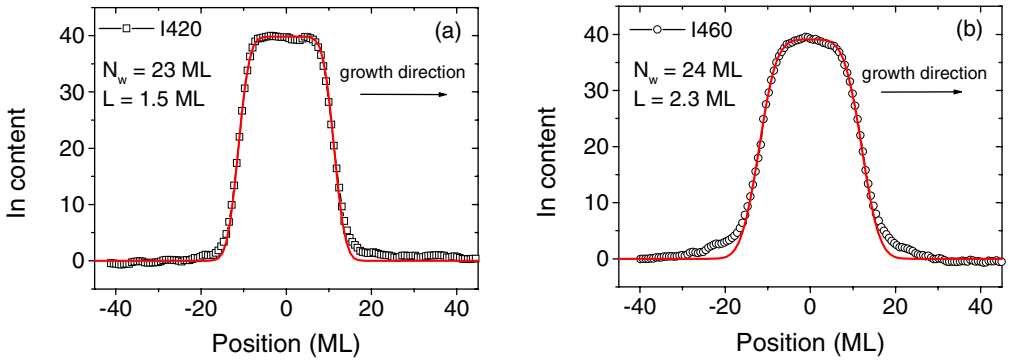

Figure 5. Experimental indium distribution from (a) I420 and (b) I460 and its description by error functions.

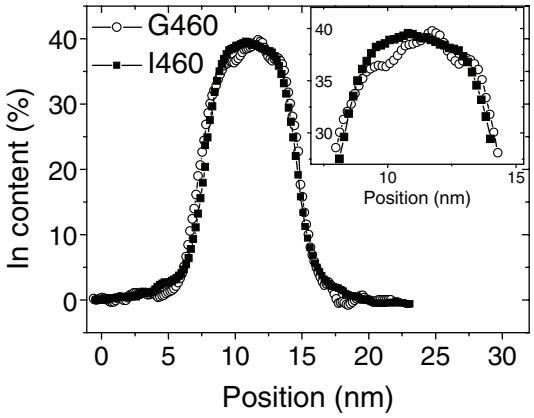

Figure 6. Experimental In profiles for the samples with/without N in the QW at 460 °C. No indium segregation is detected for the (In,Ga)As QW.

Finally, according to the [In] and [N] distribution shown in figure 2(d), the strong N accumulation at the interfaces would increase In segregation there. The question whether the phase separation tendency affects indium segregation or whether it is indium segregation that affects the phase separation tendency then arises. Preliminary experiments performed on samples grown at constant T_g but under different As fluxes, show that the As pressure has no detectable effect on the morphological instabilities associated with the composition modulations [27, 31] but controls indium surface segregation. Thus, the element distribution would be determined by surface segregation, the latter affecting the phase separation tendency. A similar influence of surface segregation on phase separation has been already reported for the metastable In(As,Sb) and (In,Ga)N systems [35, 36]. At present, additional work is in progress to further clarify this point.

4. Conclusions

We found for the first time direct evidence that the presence of nitrogen in the (Ga,In)(N,As) QW enhances indium segregation when compared to the nitrogen-free (In,Ga)As QW grown under similar conditions in the T_g range from 420 to 460 °C. As a consequence of the phase

separation tendency, this asymmetry in indium distribution produces strong fluctuations in the nitrogen content. The occurrence of In segregation in (Ga,In)(N,As) QWs should be considered in the design of devices based on this alloy, as it critically influences the potential profile and therefore the energy levels and corresponding emission wavelength.

Acknowledgments

We acknowledge Mrs A Pfeiffer for technical assistance and Dr Kui Du for his assistance with the LADIA software. This work was carried out, in part, within the framework of the *EU FP6 Fast Access* Project.

References

[1] Tournié E and Gil B 2002 Mixed III-V-N semiconductors: a challenge for tomorrow? *Low Dimensional Nitride Semiconductors* ed B Gil (New York: Oxford University Press) chapter 15 p 415
[2] Kent P R C and Zunger A 2001 Evolution of III-V nitride alloy electronic structure: the localized to delocalized transition *Phys. Rev. Lett.* **86** 2613–6
[3] Kondow M, Uomi K, Niwa A, Kitatani T, Watahiki S and Yazawa Y 1996 GaInNAs: a novel material for long-wavelength-range laser diodes with excellent high-temperature performance *Japan J. Appl. Phys.* **35** 1273–5
[4] Wei S-H and Zunger A 1996 Giant and composition-dependent optical bowing coefficient in GaAsN alloys *Phys. Rev. Lett.* **76** 664–7
[5] Shan W, Walukiewicz W, Ager J W III, Haller E E, Geisz J F, Friedman D J, Olson J M and Kurtz S R 1999 Band anticrossing in GaInNAs alloys *Phys. Rev. Lett.* **82** 1221–4
[6] Jaschke G, Averbeck R, Geelhaar L and Riechert H 2005 Low threshold InGaAsN/GaAs lasers beyond 1500 nm *J. Cryst. Growth* **278** 224–8
[7] Ho I and Stringfellow G B 1997 Solubility of nitrogen in binary III–V systems *J. Cryst. Growth* **178** 1–7
[8] Neugebauer J and Van de Walle C G 1995 Electronic structure and phase stability of $GaAs_{1-x}N_x$ alloys *Phys. Rev.* B **51** 10568–71
[9] Moison J M, Guille C, Houzay F, Barthe F and Van Rompay M 1989 Surface segregation of third-column atoms in group III-V arsenide compounds: ternary alloys and heterostructures *Phys. Rev.* B **40** 6149–62
[10] Muraki K, Fukatsu S, Shiraki Y and Ito R 1992 Surface segregation of In atoms during molecular beam epitaxy and its influence on the energy levels in InGaAs/GaAs quantum wells *Appl. Phys. Lett.* **61** 557–9
[11] Fischer M, Gollub D, Reinhardt M, Kamp M and Forchel A 2003 GaInNAs for GaAs based lasers for the 1.3 to 1.5 μm range *J. Cryst. Growth* **251** 353–9
[12] Liu H F, Xiang N and Chua S J 2006 Influence of N incorporation on In content in GaInNAs/GaNAs quantum wells grown by plasma-assisted molecular beam epitaxy *Appl. Phys. Lett.* **89** 071905
[13] Grillo V, Albrecht M, Remmele T, Strunk H P, Egorov A Y and Riechert H 2001 Simultaneous experimental evaluation of In and N concentrations in InGaAsN quantum wells *J. Appl. Phys.* **90** 3792–8
[14] Pavelescu E-M, Slotte J, Dhaka V D S, Saarinen K, Antohe S, Cimpoca G and Pessa M 2006 On the optical crystal properties of quantum-well GaIn(N)As/GaAs semiconductors grown by molecular-beam epitaxy *J. Cryst. Growth* **297** 33–7
[15] Bithell E G and Stobbs W M 1989 Composition determination in the GaAs/(Al,Ga)As system using contrast in dark-field transmission electron microscope images *Phil. Mag.* A **60** 39–62
[16] Du K, Rau Y, Jin-Phillipp N Y and Phillipp F 2002 Lattice distortion analysis directly from high resolution transmission electron microscopy images—the LADIA program package *J. Mater. Sci. Technol.* **18** 135–8
[17] Bierwolf R, Hohenstein M, Phillipp F, Brandt O, Crook G E and Ploog K 1993 Direct measurement of local lattice distortions in strained layer structures by HREM *Ultramicroscopy* **49** 273–85

[18] Vurgaftman I and Meyer J R 2003 Band parameters for nitrogen-containing semiconductors *J. Appl. Phys.* **94** 3675–96
[19] Doyle P A and Turner P S 1968 Relativistic Hartree-Fock x-ray and electron scattering factors *Acta Crystallogr.* A **24** 390–7
[20] Glas F 2004 The effect of the static atomic displacements on the structure factors of weak reflections in cubic semiconductor alloys *Phil. Mag.* **84** 2055–74
[21] Rosenauer A, Schowalter M, Glas F and Lamoen D 2005 First-principles calculations of 002 structure factors for electron scattering in strained $In_xGa_{1-x}As$ *Phys. Rev.* B **72** 085326
[22] Cagnon J, Buffat P A, Stadelmann P A and Leifer K 2003 Theoretical and experimental limits of quantitative analysis of strain and chemistry of InGaAs/GaAs layers using (200) dark-field TEM imaging *Inst. Phys. Conf. Ser.* **180** 203–6
[23] Patriarche G, Largeau L, Harmand J-C and Gollub D 2004 Morphology and composition of highly strained InGaAs and InGaAsN layers grown on GaAs substrate *Appl. Phys. Lett.* **84** 203–5
[24] Cerva H 1991 Transmission electron microscopy of heteroepitaxial layer structures *Appl. Surf. Sci.* **50** 19–27
[25] Brandt O, Waltereit P and Ploog K H 2002 Determination of strain state and composition of highly mismatched group III-nitride heterostructures by x-ray diffraction *J. Phys. D: Appl. Phys.* **35** 577
[26] Chauveau J M, Trampert A, Ploog K H and Tournié E 2004 Nanoscale analysis of the In and N spatial redistributions upon annealing of GaInNAs quantum wells *Appl. Phys. Lett.* **84** 2503–5
[27] Kong X, Trampert A, Tournié E and Ploog K H 2005 Decomposition in as-grown (Ga,In)(N,As) quantum wells *Appl. Phys. Lett.* **87** 171901
[28] Peng C S, Pavelescu E-M, Jouhti T, Konttinen J, Fodchuk I M, Kyslovsky Y and Pessa M 2002 Suppression of interfacial atomic diffusion in InGaNAs/GaAs heterostructures grown by molecular-beam epitaxy *Appl. Phys. Lett.* **80** 4720–2
[29] Matthews J W and Blakeslee A E 1974 Defects in epitaxial multilayers: I. Misfit dislocations *J. Cryst. Growth* **27** 118–25
[30] Tomić O and Reilly E P 2003 Optimization of material parameters in 1.3 μm InGaAsN-GaAs lasers *IEEE Photonics Technol. Lett.* **15** 6–8
[31] Ishikawa F, Luna E, Trampert A and Ploog K H 2006 Critical parameters for the molecular beam epitaxial growth of 1.55 μm (Ga,In)(N,As) multiple quantum wells *Appl. Phys. Lett.* **89** 181910
[32] Martini S, Quivy A A, da Silva E C F and Leite J R 2002 Real-time determination of the segregation strength of indium atoms in InGaAs layers grown by molecular-beam epitaxy *Appl. Phys. Lett.* **81** 2863–65
[33] Litvinov D, Gerthsen D, Rosenauer A, Schowalter M, Passow T, Feinäugle P and Hetterich M 2006 Transmission electron microscopy investigation of segregation and critical floating-layer content of indium for island formation in $In_xGa_{1-x}As$ *Phys. Rev.* B **74** 165306
[34] Kim K and Zunger A 2001 Spatial correlations in GaInAsN alloys and their effects on band-gap enhancement and electron localization *Phys. Rev. Lett.* **86** 2609–12
[35] Miyoshi H, Suzuki R, Amano H and Horikoshi Y 2002 Sb surface segregation effect on the phase separation of MBE grown InAsSb *J. Cryst. Growth* **237–9** 1519–24
[36] Chen H, Feenstra R M, Northrup J E, Zywietz T and Neugebauer J 2000 Spontaneous formation of indium-rich nanostructures on InGaN(0001) surfaces *Phys. Rev. Lett.* **85** 1902–5